Design and manufacturing of Magnets for e-beam interaction with Ultrafast High Power Laser beam

Oscar Situ[1], Viviana Vladutescu[1], Mikhail Polyanskiy[2], William Li[2], Vikas Teotia[3], Marcus Babzien[2], Dismas Choge[2], Li Geng[1], Tianyi Zhao[1], Tahsinur Rahman[1], Brandon Palencia[1], Joseph Rukaj[1], Jorge Chavez[1], Mithila Islam[1], Lufeng Leng[1], Giovanni Ossola[1], Mark Palmer[2]

[1] Department of Electrical and Telecommunications Engineering Technology, CUNY New York City College of Technology, Brooklyn, NY, 11201, USA
[2] Accelerator Test Facility, Brookhaven National Laboratory, Upton, NY, 11973, USA; [3] Superconducting Magnet Division, Brookhaven National Laboratory, Upton, NY, 11973, USA

ABSTRACT

Magnet modeling with Opera3D and Rat-GUI was used to analyze nonlinear materials, varying current densities, and constructing models for a window magnet and Canted-Cosine Theta (CCT) coil magnet; of which was later fabricated with BNL's Direct Wind machine. In the context of UED, such magnets are critical for shaping and steering electron beams, how different beam parameters and components affect beam dynamics were analyzed using General Particle Tracer (GPT) and later compared with real beamline performance. Meanwhile, optical lasers were also simulated using software such as 3DOptix and SNLO. Optical lasers and electron beams are deeply intertwined in modern ultrafast and accelerator science. Lasers can generate, manipulate, or temporally synchronize electron beams, while electrons can act as probes or even sources of light through laser-beam interactions.

INTRODUCTION

Since the early 20th century, particle accelerators have been central to groundbreaking scientific discoveries and technological advancements. To sustain and advance this legacy, it is essential to cultivate the next generation of researchers in the fundamental physics, engineering, and applied technologies underlying accelerator science [1][2].

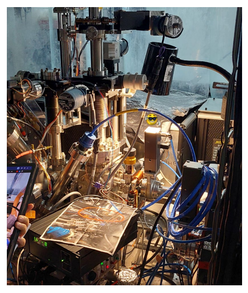

Fig. 1 UED Electron Beamline

THEORY / BACKGROUND

Examples of beam simulation with General Particle Tracer (GPT), with varying beam parameters and beam changing components. Beam size can be represented by:

$$\varepsilon = x'^2 + 2\alpha x x' + \beta x'^2 \quad (1)$$

$$\varepsilon_g = \sqrt{\langle x^2\rangle\langle x'^2\rangle - \langle xx'\rangle^2} \quad (2)$$

where ε is the area occupied by beam particles in an *x* (position), *x'* (momentum) plane, and γ, α, β are Twiss parameters, where α represents the tilt of an ellipse in a phase space plot, β the width, and γ is related to the focusing strength of the beamline (and is dependent on α and β) [2].

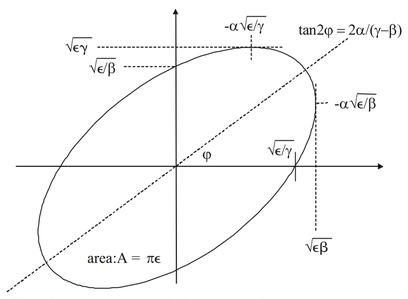

Fig. 2 momentum (x') vs position (x) plot in phase space [2]

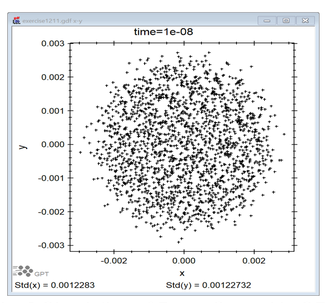

Fig. 3 Simulation of Beam Spread in GPT

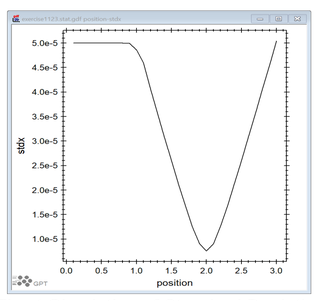

Fig. 4 Simulation of Standard Deviation vs Position graph for focusing in GPT

Fundamental to the operation of such electron beamlines are electromagnetic coils and their magnetic fields. They are the main driver for the steering, focusing, and manipulating of charged particles via Lorentz force and related electromagnetic principles [2]. Lorentz force is described as:

$$\vec{F} = q(\vec{E} + \frac{1}{c}\vec{v} \times \vec{B}) \quad (3)$$

where *F* is force generated when a particle of charge *q*, with velocity *v* is moving through a magnetic field *B* and or with an electric field *E*. This is the main driver behind magnets and electromagnetic force.

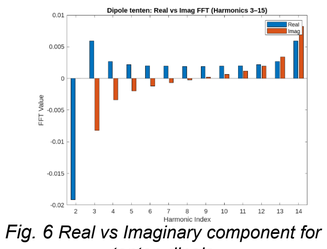

Fig. 6 Real vs Imaginary component for tenten dipole

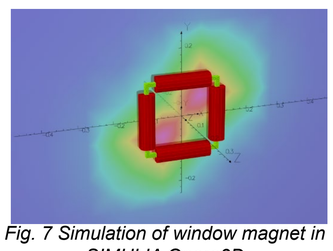

Fig. 7 Simulation of window magnet in SIMULIA Opera3D

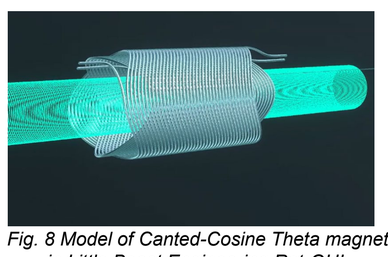

Fig. 8 Model of Canted-Cosine Theta magnet in Little Beast Engineering Rat-GUI.

Window magnets such as the one shown in figure 4, are typically used in places such as electron beams with availability for dipole and quadrupole configurations based on current flow. Dipole magnets will shift the particle beam in a direction, quadrupole magnets focus one axis while defocusing the other.

A canted-cosine theta design as shown in figure 5 was chosen for the fabrication of a magnetic coil due to its simplistic construction, high-quality magnetic fields, and overall stability under training and performance.

The CCT coil was fabricated with BNL's Direct Wind Machine using two aluminum tubes (4" Inner, 4.5" Outer, 1/8" Thickness, 1/8" Gap between, 12" Length). An epoxy subtract was layered on top, and then wound with Nb-Ti wire. Later, a layer of epoxy tape, LV24 Stycast, and Teflon tape was applied on top of the coil in that order. It is left to dry for 24 hours before being cured at 249°F for 90 mins, and then cured again at 350°F for another 90 mins.

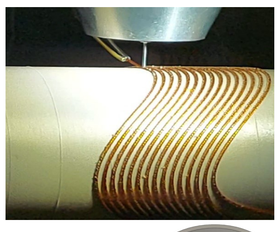

a.

End cap components also were designed by fellow intern and colleague, Joseph Rukaj, to constrain the coil at fixed positions and provide structural support.

Fig. 9 a. CCT Coil fabrication with Direct Wind Machine
b. End cap component design

b.

Related and used in certain types of analysis, optical lasers are stimulated emissions of radiation that can deliver high amounts of energy in the form of coherent beams of light [4].

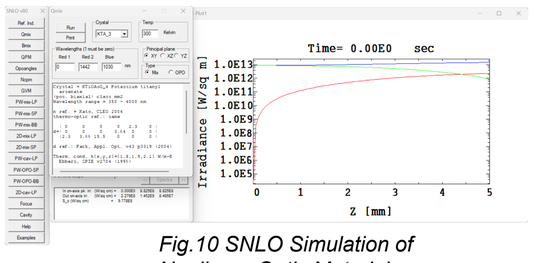

Fig.10 SNLO Simulation of Nonlinear Optic Materials

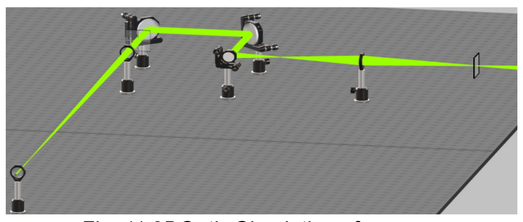

Fig. 11 3DOptix Simulation of an optical setup

RESULTS

This section presents the experimental results and evaluates their agreement with corresponding simulation data.

a.

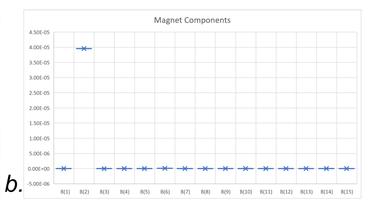

b.

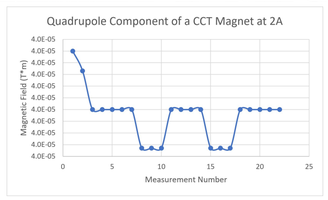

c.

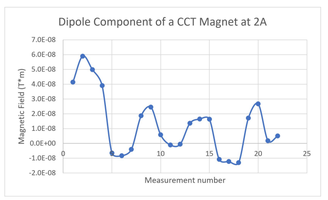

d.

e.

Fig. 12 a. Window and CCT magnet being tested, b. magnet components, c. quadrupole components, d. dipole components, e. Rat-GUI component computations

From the data obtained from using the rotating coil magnetometer to gauge magnetic field, the magnet is mostly quadrupolar as shown in fig.12(d).

This corresponds with the simulations of fig. 12(e) done in Rat-GUI

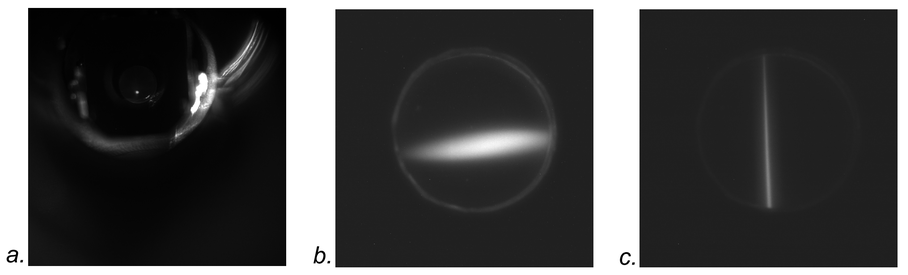

a. *b.* *c.*

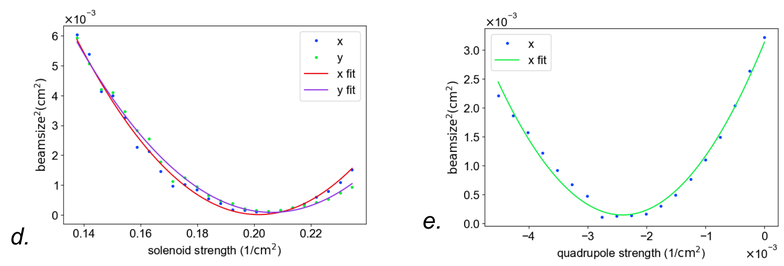

d. *e.*

Fig. 13 a. Solenoid Scan@167A, b. Quadrupole Scan@0.450A, c. Quadrupole scan@-.450A
d. plot of beam size over solenoid strength, e. plot of beam size over quadrupole strength

Solenoid and quadrupole scan of the e-beam

As current increases, so does magnetic field of the magnets.

Figure 10(d)(e) shows that there must be specific current and magnetic field for the beam size to be focused at a certain point. Similar to what was seen in figure 4.

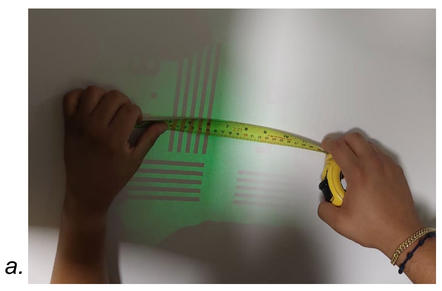

a.

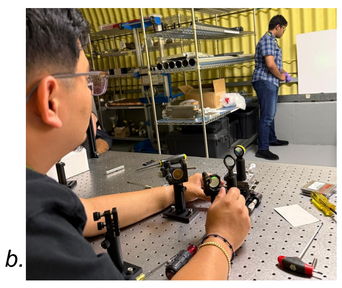

b.

Fig. 14 a. Measuring image size from imaging/magnification setup, b. setting up the beam alignment.

Using a similar optical setup to the one shown in Fig. 11, a lense with an image is used to compare object size and image size.

Equations used:

$$m = \frac{h_i}{h_o} = -\frac{d_i}{d_o} \quad (4)$$

$$\frac{1}{f} = \frac{1}{d_o} + \frac{1}{d_i} \quad (5)$$

DISCUSSION / CONCLUSION

The rotating coil magnetometer measurements agree with the SCM simulations in Rat GUI and OPERA. As shown in Figure 10(d), the beam reaches its minimum size at a specific quadrupole strength, indicating optimal focusing. This observation is consistent with the behavior previously illustrated in Figure 3. Additionally, as the quadrupole polarity reverses between Figures 10(b) and 10(c), the focusing and defocusing axes are switched, exactly what we expect from quadrupole magnetic fields. The experimental results aligned well with theoretical and simulation predictions, reinforcing our understanding and supporting the continued advancement of accelerator science and technology. This presentation includes "No export controlled" work.

References

[1] S. Tazzari, "Short History of Particle Accelerators Short History of Particle Accelerators," Universita di Roma, CERN, 2006. [Online]. Available: https://cas.web.cern.ch/sites/default/files/lectures/zakopane-2006/tazzari-history.pdf
[2] H. Wiedemann, "Introduction to Accelerator Physics," *Graduate Texts in Physics*, pp. 3–41, 2015, doi: https://doi.org/10.1007/978-3-319-18317-6_1.
[3] D. Filippetto *et al*., "Ultrafast electron diffraction: Visualizing dynamic states of matter," vol. 94, no. 4, Dec. 2022, doi: https://doi.org/10.1103/revmodphys.94.045004.
[4] V. Chvykov, "High-Power Lasers," *Encyclopedia*, vol. 4, no. 3, pp. 1236–1249, Aug. 2024, doi: https://doi.org/10.3390/encyclopedia4030080.

Acknowledgements

This work is supported by the DOE Office of Science through the SESAPARD/RENEW Grant: "Science and Engineering Apprenticeship Program in Accelerator Science and Technology", DE-SC0025742 and in part by Office of Workforce Development for Teachers and Scientists (WDTS). Additionally, we would like to acknowledge the invaluable guidance and support of Jason Becker, John Escallier, Christopher Tamargo, Michael Hartsough, Michael Anerella from the Superconducting Magnet Division, Jhair Alzamora, Paul Jacob, Karl Kusche, Anusorn Lueangaramwong, and Miguel Long from the Accelerator Facilities Division at Brookhaven National Laboratory, as well as the rest of the scientists, engineers, and technicians at the Accelerator Test Facility and Superconducting Magnet divisions for the continued support in this work. Their collective expertise and encouragement were essential to every stage of this work—from early design discussions and simulation troubleshooting to prototype fabrication and testing.

U.S. DEPARTMENT of ENERGY
NEW YORK CITY COLLEGE OF TECHNOLOGY CUNY
www.bnl.gov
SESAPARD NYCCT CUNY DOE BNL RENEW PARTICLE ACCELERATORS SCIENCE AND TECHNOLOGY
Brookhaven National Laboratory